Arthropod Structure & Development 42 (2013) 407–423

Contents lists available at SciVerse ScienceDirect

Arthropod Structure & Development

journal homepage: www.elsevier.com/locate/asd

Phylogenetic affinities of *Phobetinus* to other pirate spider genera (Araneae: Mimetidae) as indicated by spinning field morphology

Mark A. Townley [a,*], Danilo Harms [b,c], Suresh P. Benjamin [d,e]

[a] Research Computing & Instrumentation, University of New Hampshire, Rudman Hall, 46 College Road, Durham, NH 03824, USA
[b] School of Animal Biology, University of Western Australia, 35 Stirling Highway, Crawley, Western Australia 6009, Australia
[c] Department of Terrestrial Zoology, Western Australian Museum, Locked Bag 49, Welshpool DC, Western Australia 6986, Australia
[d] Institute of Fundamental Studies, Hantana Road, Kandy 20000, Sri Lanka
[e] Zoological Research Museum Alexander Koenig, Adenauerallee 160, 53113 Bonn, Germany

ARTICLE INFO

Article history:
Received 19 February 2013
Accepted 29 April 2013

Keywords:
Australomimetus
Ero
Mimetus
Silk gland spigots
Spinnerets
Sri Lanka

ABSTRACT

Spinnerets from *Phobetinus sagittifer* and an undescribed *Phobetinus* species were examined by scanning electron microscopy to gain a better understanding of this genus' relationships to other genera in the family Mimetidae. Consistent with placement of *Phobetinus* in Mimetinae, females possessed two synapomorphies of this subfamily; enlarged cylindrical silk gland spigots with domed shafts and a single cylindrical spigot per posterior lateral spinneret (PLS). Spinning field features overall suggest *Phobetinus* is most closely related to *Mimetus*, followed by *Australomimetus*, then *Ero*. A possible synapomorphy of a clade including *Mimetus* and *Phobetinus* is a pair of modified piriform silk gland spigots on each anterior lateral spinneret of adult males located adjacent to the secondary major ampullate silk gland tartipore. These spigots were present in *P. sagittifer*; however, similarly positioned spigots in the undescribed species were not obviously modified (i.e., wider or with larger openings relative to the other piriform spigots). Close affinity to *Mimetus* was also indicated by tartipore-accommodated PLS aciniform silk glands in both *Phobetinus* species. These have been consistently observed in *Mimetus*, but not in *Australomimetus* or *Ero*. Somatic and genitalic drawings of *P. sagittifer* are provided to aid identification and similarities are noted between male pedipalps of *Mimetus* and *Phobetinus*.

1. Introduction

Spiders of the family Mimetidae are commonly called pirate spiders because of their proclivity for feeding on other spiders. They sometimes employ a tactic of web invasion coupled with aggressive behavioral mimicry to lure and attack their spider prey (Czajka, 1963; Jackson and Whitehouse, 1986). Mimetids do not build prey capture webs (Hickman, 1967; Heimer, 1986), nor do they possess two synapomorphies of the superfamily Araneoidea, aggregate silk glands (Ag) and flagelliform silk glands (Fl) (Coddington, 1986), used by ecribellate orb web builders to form sticky capture spirals (Peters, 1987). Nevertheless, recent phylogenetic analyses of DNA sequence data, alone or in combination with morphological/ethological data, hypothesize a sister-group relationship between mimetids and the orb-web-building family Tetragnathidae, within the Araneoidea (Blackledge et al., 2009; Dimitrov and Hormiga, 2011; Dimitrov et al., 2012).

Mimetidae currently comprises 156 described species in 13 genera (Platnick, 2013), divided among four subfamilies: Gelanorinae, Melaenosiinae, Mimetinae, and Oarcinae (Mello-Leitão, 1935; Platnick and Shadab, 1993). The family composition, however, is in flux: based on molecular data, Dimitrov et al. (2012) have recently proposed transferring Oarcinae to the orb-web-building family Araneidae and it is also doubtful that Melaenosiinae are mimetids (Platnick and Shadab, 1993; Harms and Dunlop, 2009). The subfamily Mimetinae contains the bulk of described mimetid species (128), at present divided among seven genera: *Arocha* Simon, 1893, *Australomimetus* Heimer, 1986, *Ermetus* Ponomarev, 2008, *Ero* C.L. Koch, 1836, *Mimetus* Hentz, 1832, *Phobetinus* Simon, 1895, and *Reo* Brignoli, 1979 (Harms and Harvey, 2009b). Affinities among these genera are uncertain, in part because of insufficient morphological data (Harms and Dunlop, 2009). Spinneret morphology, for example, has been examined by scanning electron microscopy (SEM) in representatives of only the three largest mimetine genera (*Mimetus*, *Ero*, *Australomimetus*), prompting recommendations that the smaller genera be likewise examined to promote a better

* Corresponding author. University of New Hampshire, Rudman Hall, 46 College Road, Durham, NH 03824, USA. Tel.: +1 603 862 0632.
E-mail addresses: mtownley@cisunix.unh.edu (M.A. Townley), d.harms01@googlemail.com (D. Harms), suresh.benjamin@gmail.com (S.P. Benjamin).

1467-8039/$ – see front matter © 2013 Elsevier Ltd. All rights reserved.
http://dx.doi.org/10.1016/j.asd.2013.04.003

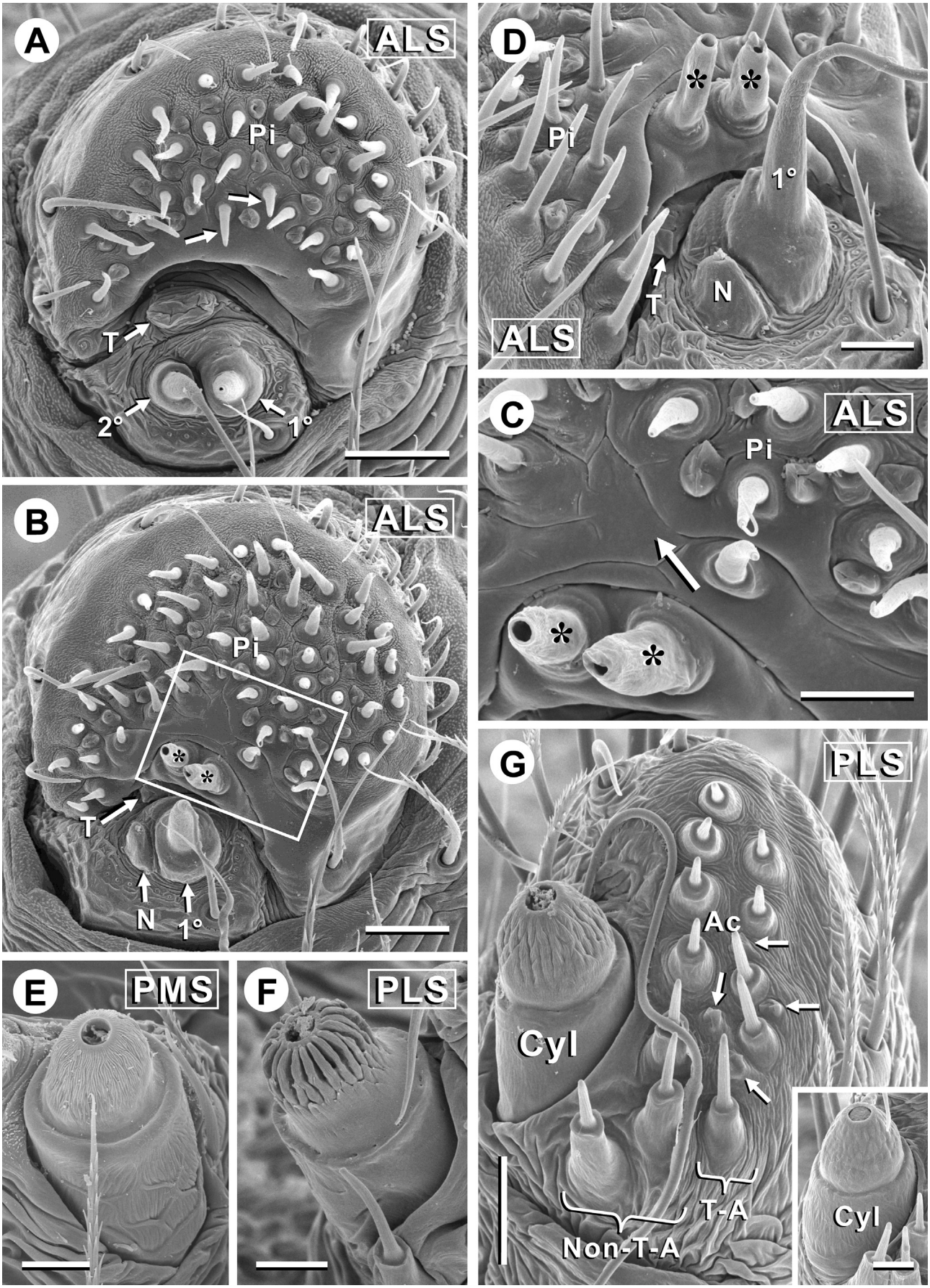
A
ALS
Pi
T
2°
1°
B
ALS
Pi
T
N
1°
D
Pi
1°
T
N
ALS
C
ALS
Pi
G
PLS
Ac
Cyl
T-A
Non-T-A
Cyl
E
PMS
F
PLS

understanding of mimetine relationships (Platnick and Shadab, 1993; Harms and Harvey, 2009b). Here we provide observations of spinning field morphology in *Phobetinus*, a poorly known genus not investigated in detail before. Given results from earlier studies, certain spinning field features in this genus were of particular interest, as detailed in the following paragraphs.

Based on SEM scans of spinnerets from representatives of Mimetinae, Gelanorinae, and Oarcinae, Platnick and Shadab (1993) proposed a synapomorphy of the Mimetinae: enlarged cylindrical silk gland (Cyl) spigots with substantial bases and domed, large-aperture, incised (grooved) shafts (see Sect. 2.4). This morphology applied to the two mimetine genera they examined, *Ero* (Fig. 1F) and *Mimetus* (Fig. 1G) (see also Schütt, 2000; Griswold et al., 2005; Townley and Tillinghast, 2009), and was later confirmed also in *Australomimetus*, except that their Cyl spigot shafts were not incised (Fig. 1E) (Harms and Harvey, 2009a, 2009b; Townley and Tillinghast, 2009).

Though not unique within the Araneoidea (Griswold et al., 1998; Griswold, 2001; Lopardo and Hormiga, 2007; Miller, 2007), a second apparent synapomorphy of the Mimetinae that has not, to our knowledge, been explicitly stated as such, is the presence of just a single Cyl spigot on each posterior lateral spinneret (PLS) in females (Fig. 1G) (see also Platnick and Shadab, 1993; Schütt, 2000; Griswold et al., 2005; Harms and Harvey, 2009a, 2009b; Townley and Tillinghast, 2009). This is in contrast to the two Cyl spigots per PLS that are plesiomorphically present in Araneoidea (Griswold et al., 1998) and that have been observed in those Gelanorinae, Oarcinae, and *Arkys* examined to date (Platnick and Shadab, 1993) [the latter genus is currently placed in Araneidae (Scharff and Coddington, 1997; Platnick, 2013), but recent phylogenetic analyses indicate a sister-group relationship to Tetragnathidae or Mimetidae (Blackledge et al., 2009; Dimitrov and Hormiga, 2011; Dimitrov et al., 2012)].

A proposed synapomorphy of *Mimetus* is a pair of spigots on each anterior lateral spinneret (ALS) of adult males that appear to serve modified piriform silk glands (MoPi) and sit adjacent and anterior to the secondary (2°) major ampullate silk gland (MaA) tartipore (see Sect. 2.4), separated from the typical piriform silk gland (Pi) spigots by at least a cuticular fold (Fig. 1B, asterisks) (Townley and Tillinghast, 2009). These spigots have wider apertures and, often, wider and less tapered shafts than the surrounding typical Pi spigots (Fig. 1C, D, asterisks) (Griswold et al., 2005; Townley and Tillinghast, 2009). MoPi spigots have not been discerned in adult male *Australomimetus* (3 examined species), but some adult male *Ero* (2 of 5 species) have been found to possess a pair of more subtle MoPi spigots on each ALS (Townley and Tillinghast, 2009). These had wider openings (though not markedly wider shafts) than surrounding Pi spigots, but in contrast to *Mimetus* MoPi spigots, were not located next to the 2° MaA tartipore and were not set off from the typical Pi spigots by a cuticular fold (Fig. 14C, D and 15A–C in Townley and Tillinghast, 2009).

Also found to be variable among mimetines, and thus with the potential to help elucidate inter- or intra-generic relationships, is the occurrence of 1) tartipore-accommodated (T-A; see Sect. 2.4) aciniform silk glands (Ac) emptying on the PLS and 2) 2° minor ampullate silk glands (MiA) in juveniles (Townley and Tillinghast, 2009). The former are indicated externally by Ac tartipores on the PLS (Fig. 1G), the latter by a 2° MiA tartipore and a 2° MiA spigot on each posterior median spinneret (PMS) of juveniles, with the spigot replaced by a nubbin (see Sect. 2.4) in adults.

Though mimetids lack the Ag and Fl present in most araneoids, occasionally, in specimens of juvenile male and female *Mimetus notius* Chamberlin 1923, single putative nubbins have been observed on PLS that potentially represent phylogenetic vestiges of Ag or Fl spigots (Townley and Tillinghast, 2009). These have not as yet been observed in *Australomimetus* or *Ero*, but they may be present in other mimetine representatives.

Phobetinus currently includes just two described species, both endemic to eastern Asia, the type species *Phobetinus sagittifer* Simon, 1895 and *Phobetinus investis* Simon, 1909 (Platnick, 2013). In this paper we present SEM observations on the spinning fields of *P. sagittifer* and an undescribed species from Papua New Guinea that we refer to as *Phobetinus* sp. PNG. Following from the aforementioned findings of previous studies, specific goals were to 1) confirm the presence of enlarged, rotund Cyl spigots in adult females that occur as singles on each PLS (as well as on each PMS), 2) determine if Cyl spigot shafts are grooved, as in *Ero* and *Mimetus*, or not, as in *Australomimetus*, 3) determine if MoPi spigots like those in *Mimetus*, or perhaps a less obvious version as in some *Ero*, are present in adult male *Phobetinus*, 4) look for external evidence of 2° MiA in juveniles, 5) examine PLS for external evidence of T-A Ac, and 6) examine PLS for potential vestiges of Ag or Fl spigots.

Apart from Simon's (1895) drawing of the unusual dorsal abdominal setae of *P. sagittifer*, the only published somatic and genitalic diagrams of this species of which we are aware are those in Brignoli (1972). In our examinations of *P. sagittifer*, however, we noted some discrepancies with these drawings even though our specimens matched the lectotypes used by Brignoli when compared directly. We therefore present here additional habitus and copulatory organ representations of *P. sagittifer* and, for comparison, male palps from representative *Australomimetus*, *Ero* and *Mimetus*. These illustrations also provide a second, independent line of evidence in the process of relating *Phobetinus* to other mimetine genera.

2. Materials and methods

2.1. Study species

Three individuals of *P. sagittifer* were hand collected in Sri Lanka (Riverston, Knuckles Range, Matale District, Central Province; adult ♂-1, 07°32′36″N, 80°45′13″E, 800 m, 05-I-2010, S. P. Benjamin, S. Batuwita, P. M. H. Sandamali; adult ♂-2 and adult ♀, 07°31′17″N, 80°44′04″E, 1220 m, 02-II-2010, S. Batuwita, P. M. H. Sandamali et al.) and used for spinneret studies. They have been deposited at the Zoological Research Museum Alexander Koenig, Bonn, Germany (ZFMK); adult ♂-1, ZFMK Ar 8872; adult ♂-2, ♀, ZFMK Ar 8873. Two additional *P. sagittifer* specimens (adult ♂, ♀, Deenston, Knuckles Range, Matale District, Central Province, Sri Lanka, 07°20′10″N, 80°51′31″E, 1120 m, 10-III-1998, S. P. Benjamin) were

Fig. 1. Spinnerets of *Mimetus puritanus*, *Australomimetus auriocculatus* (Hickman 1929), and *Ero tuberculata*. A–D. Right ALS, male *M. puritanus*, Andersonville, TN, USA. A. Penultimate instar cuticle (on final exuvium shed). B. Adult cuticle from the same individual. Unlabeled arrows in (A) point to the two non-T-A Pi spigots, as determined by matching Pi spigots in (A) with Pi tartipores in (B). C. Boxed region in (B), magnified, with MoPi spigots indicated by asterisks. Arrow to bare patch of cuticle referred to in Sect. 4.2. D. Same ALS as in (B, C), from more posterior and tilted perspective. E–F. Adult female Cyl spigots. E. Left PMS, *A. auriocculatus*. F. Left PLS, *E. tuberculata*. Cyl spigot shaft in (E) is striated, but not incised; that in (F) is deeply incised. G. Left PLS, adult female *M. puritanus*, Epping, NH, USA. Left column of 7 Ac spigots, close to Cyl spigot (Cyl), serve non-T-A Ac (Non-T-A); right column of 5 Ac spigots serve T-A Ac (T-A). Arrows to Ac tartipores. Cyl spigot shaft is shallowly incised. Inset shows Cyl spigot (Cyl) on left PLS from another adult female *M. puritanus*, Fryeburg, ME, USA. Shaft is not clearly incised (at most, no more than in some *A. auriocculatus* specimens; see Fig. 18G, 23C in Townley and Tillinghast, 2009). Anterior at right, mesal at bottom in (A–D); anterior right, mesal top in (E); anterior left, mesal bottom in (F, G). Scale bars: A, B, G 20 μm; C–F, G inset 10 μm. 1°, 1° MaA spigot; 2°, 2° MaA spigot; Ac, Ac spinning field; N, 2° MaA nubbin; Pi, Pi spinning field; T, 2° MaA tartipore.

used to prepare the copulatory structure and habitus illustrations in Figs. 7D, 8, and 9A and have been deposited at the Muséum d'Histoire naturelle, Geneva, Switzerland (MHNG). Dr. Christine Rollard, Muséum national d'Histoire naturelle, Paris, France (MNHN), kindly loaned the *P. sagittifer* lectotypes illustrated by Brignoli (1972) (MNHN Inventory AR14618, Object 16304), from which the male pedipalp images in Fig. 7A–C were prepared (the epigynum from the female lectotype is in pieces and was therefore not re-illustrated).

Three individuals of *Phobetinus* sp. PNG were collected in Papua New Guinea (adult ♂, ♀, juvenile (apparently penultimate instar) ♀, Camps 1 & 2, Muller Range, Western Province, 05°40'S, 142°18'E, 1425–1660 m, 04-14-IX-2009, I. Agnarsson) and their spinnerets were prepared for SEM. They have been deposited at the Western Australian Museum, Perth, Australia (WAM); adult ♀, WAM T129161; adult ♂, WAM T129162; penultimate instar ♀, WAM T129163.

The male pedipalps illustrated in Fig. 9B–D for comparative purposes were from: *Mimetus syllepsicus* Hentz, 1832 (Lake Istokpoga, Florida, USA, 10–20 m, 28-II-1951, A. M. Nadler, American Museum of Natural History, New York, USA); *Australomimetus* sp. (Manusela National Park, Ceram, Maluku [Moluccas] Islands, Indonesia, 380–400 m, 26-29-XI-1996, M. Kuntner et al., Museum für Naturkunde, Berlin, Germany, ZMB 32724); and *Ero aphana* (Walckenaer, 1802) (Jarrahdale, Western Australia, 32°57′S, 116°27′E, 250 m, 03-IX-2006, D. Harms, M. G. Rix, WAM T66695).

2.2. Examination of spinnerets

Spinnerets from ethanol-preserved specimens of *P. sagittifer* and *Phobetinus* sp. PNG were prepared for SEM as follows. Fine spring scissors were used to transect the abdomen just anterior of the spinnerets. The spinnerets were immersed in a 2X-strength SDS-PAGE running buffer (Novex Tris-glycine SDS; Life Technologies Corp. LC2675) at 4 °C for at least 3 days, following which forceps were used to remove as much remaining soft tissue from the cuticle as possible. In an attempt to reduce the likelihood of examining collapsed spinnerets, each spinneret in the set, while still immersed in the SDS-containing buffer, was pulled down onto the tip of a pin of appropriate size that projected upwards from a wax surface in a Petri dish (Townley and Tillinghast, 2009). The spinnerets were then dehydrated through an ethanol series (30%, 50%, 70%, 85%, 95%, twice in 100%; at least 1 day in each), critical-point dried, mounted on SEM stubs, sputter-coated, and examined by SEM as described previously (Townley and Tillinghast, 2003, 2009).

2.3. Examination of pedipalps

Specimens used for illustrations were preserved in 70–75% ethanol and general morphological examinations were carried out using a Leica MZ16A stereomicroscope. Images were taken by a Leica DFC 500 digital camera mounted on this microscope, using Leica Application Suite Version 3.6.0 software. Line drawings were made on tracing paper using printed automontage images as templates. It is noted that the pedipalps of Brignoli's (1972) adult male lectotype (MNHN AR14618, 16304) are faded and that the setae on the cymbium and tibia are broken off, so that illustrations referring to this specimen are reconstructions. To assure accuracy of the structures illustrated, a specimen in better condition (collected in 1998; MHNG) was illustrated in parallel, though it originates from a different locality in Sri Lanka than the lectotypes.

2.4. Terminology

In the spinnerets of many spiders, during the part of the molt cycle known as proecdysis, when preparations are made for ecdysis that include the formation of a new cuticle beneath the old cuticle (exoskeleton), collared openings called **tartipores** form in the new cuticle around certain silk gland ducts. The tartipores allow these ducts to remain connected to spigots on the old cuticle. Consequently, silk can be drawn from such spigots during proecdysis. These silk glands are said to be **tartipore-accommodated (T-A)**. In *Phobetinus*, as in *Mimetus* (and *Araneus*) (Townley and Tillinghast, 2009), Pi and Ac can be divided into those that are T-A and those not so accommodated (non-T-A). Without the formation of tartipores, non-T-A silk glands cannot remain connected to spigots on the old cuticle and thus cannot function during proecdysis. On the other hand, T-A glands lose their outlets (old cuticle spigots) at ecdysis and, thus, silk presumably cannot be drawn from these glands throughout the new stadium. Non-T-A glands, given downtime for re-modeling during proecdysis, including detachment from old cuticle spigots and attachment to new cuticle spigots, can potentially function in every stadium. After ecdysis, the tartipores remain visible in the new cuticle (exoskeleton) as scars of the former openings. Though our discussion of T-A and non-T-A glands is applied in this report primarily to Pi and Ac, we note that ampullate silk glands can also be divided into T-A and non-T-A; primary (1°) MaA and 1° MiA are non-T-A, 2° MaA and 2° MiA are T-A; hence references made to 2° MaA and 2° MiA tartipores as well as their identification in a number of figures.

Since the distinction between T-A and non-T-A glands is based on events that occur during molting, and adults do not molt, and since numbers of Pi/Ac spigots often increase from one stadium to the next, it may well be that some Pi/Ac of adults have never been and will never be T-A, yet, based on other evidence, are almost certainly T-A-*type* glands. In such cases, we will still consider them to be T-A Pi/Ac.

Nubbins are vestigial spigots and may be either ontogenetically vestigial (occurring where functional spigots occurred in earlier stadia) or, less often, phylogenetically vestigial (occurring where functional spigots occurred in an ancestor). They may also form consistently within a species as part of its normal development (e.g., 2° MaA and 2° MiA nubbins in adult mimetids in place of the 2° MaA and 2° MiA spigots in juveniles) or form as inconsistent developmental anomalies. We refer readers to Townley et al. (1991, 1993) and Townley and Tillinghast (2003, 2009) for further explanation and illustration of distinctions between 1° versus 2° MaA/MiA and tartipores versus nubbins, noting, however, that the 1°/2° designations for different MaA and MiA were first applied in the 1993 paper and the current consistent distinction between tartipores and nubbins was first applied in the 2003 paper.

Spigots typically consist of two segments; a proximal base and a distal, usually narrower shaft, ending in the opening through which the silk gland's products emerge.

2.5. Spinning apparatus abbreviations

1°, primary; 2°, secondary; Ac, aciniform silk gland; Ag, aggregate silk gland; ALS, anterior lateral spinneret; Cyl, cylindrical silk gland; Fl, flagelliform silk gland; MaA, major ampullate silk gland; MiA, minor ampullate silk gland; MoPi, modified piriform silk gland; Pi, piriform silk gland; PLS, posterior lateral spinneret; PMS, posterior median spinneret; T-A, tartipore-accommodated.

3. Results

The complement of spigots, tartipores, and nubbins on the spinnerets of the six examined *Phobetinus* specimens are shown in Table 1, with data from several species of *Australomimetus*, *Ero*, and *Mimetus* also presented for comparison. Spinneret micrographs

Table 1
Spigot, tartipore, and nubbin complements on spinnerets of six *Phobetinus* specimens and, for comparison, spinnerets of other Mimetinae.[a]

Species	Stage/Gender	*N*	ALS							PMS							PLS		
			1° MaA spigot	2° MaA spigot	2° MaA tartipore	2° MaA nubbin	Pi spigots	Pi tartipores	MoPi spigots	1° MiA spigot	2° MiA spigot	2° MiA tartipore[b]	2° MiA nubbin	Ac spigots	Ac tartipore	Cyl spigot	Ac spigots	Ac tartipores	Cyl spigot
Phobetinus sagittifer	Adult ♀	1	1	0	1	1	19, 17	9, 9	0	1	0	1 (AL)	1	2	0	1	7, 7	2	1
Phobetinus sagittifer	Adult ♂-1[c]	1	1	0	1	1	13, 15	10, 8	2	1	0	1 (AL)	1	2	0	0	6, 6	2	0
Phobetinus sagittifer	Adult ♂-2[c]	1	1	0	1	1	14, 16	8, 11	2	1	0	1 (AL)	1	2	0	0	6, 6	2	0
Phobetinus sp. PNG	Penult ♀	1	1	1	1	0	9, 8	4, 4	0	1	1	1 (PM)	0	3, 2	0	1	5, 5	?, 1	1
Phobetinus sp. PNG	Adult ♀	1	1	0	1	1	12, 12	7, 6	0	1	0	1 (AL)	1	?, ≥1	?	≥1,?	5, 7	1	1
Phobetinus sp. PNG	Adult ♂	1	1	0	1	1	11, 13	6, 7	0	1	0	1	0	3, 3	0	0	5, 5	1	0
Australomimetus auriculatus	Adult ♀	2	1	0	1	1	21–27	12–14	0	1	0	1 (AL)	1	2	0	1	5–6	0	1
Australomimetus auriculatus	Adult ♂	2	1	0	1	1	18–21	10–12	0	1	0	1 (AL)	1	4–6	0	0	6	0	0
Australomimetus diabolicus	Adult ♂	1	1	0	1	1	26	16	0	1	0	1 (PM)	1	2	0	0	6, 7	0	0
Australomimetus pseudomaculosus	Adult ♂	1	1	0	1	1	33, 32	?	?	1	0	1 (AL)	1	4	0	0	8, 9	0	0
Australomimetus tasmaniensis	Adult ♂	1	1	0	1	1	13, 14	?	0	1	0	0	0	2	0	0	5	0	0
Ero aphana	Penultimate instar ♂	2	1	1	1	0	9–10	4–5	0	1	1	1 (AL)	0	2	0	0	4–5	0	0
Ero aphana	Adult ♀	1	1	0	1	1	20, 19	7, 8	0	1	0	1 (L)	1	2	0	1	6	0	1
Ero aphana	Adult ♂	2	1	0	1	1	17–18	7	2[d]	1	0	1 (PM/AM)	1	2	0	0	6	0	0
Ero canionis	Adult ♂	2	1	0	1	1	13–19	5–9	0	1	0	0	0	2	0	0	7–10	0	0
Ero furcata	Adult ♀	2	1	0	1	1	18–27	8–9	0	1	0	0	0	1	0	1	5–6	0	1
Ero furcata	Adult ♂	2	1	0	1	1	19–21	9–10	0	1	0	0	0	1	0	0	4–5	0	0
Ero leonina	Adult ♂	1	1	0	1	1	16, 18	7, 9	0	1	0	0	0	1	0	0	4	0	0
Ero tuberculata	Adult ♀	2	1	0	1	1	25–27	11–12	0	1	0	0	0	2	0	1	5–11	0	1
Ero tuberculata	Adult ♂	1	1	0	1	1	24, 25	?, 14	2[d]	1	0	0	0	2	0	0	10	0	0
Mimetus notius	5th instar adult ♀	4	1	0	1	1	30–44	19–23	0	1	0	1 (AL)	1	4	0	1	13–15	4–7	1
Mimetus notius	5th instar adult ♂	5	1	0	1	1	28–42	17–21	2	1	0	1 (AL)	1	4	0	0	10–14	3–6	0
Mimetus notius	6th instar adult ♀	2	1	0	1	1	45–49	27–29	0	1	0	1 (PM)	1	4	0	1	14–16	5–7	1
Mimetus notius	6th instar adult ♂	1	1	0	1	1	37, 35	23, 26	2	1	0	1 (PM)	1	3	0	0	15, ?	?	0
Mimetus puritanus	5th instar adult ♀	5	1	0	1	1	28–48	15–22	0	1	0	1 (AL)	1	3–4	0	1	11–14	4–5	1
Mimetus puritanus	5th instar adult ♂	2	1	0	1	1	32–42	16–21	2	1	0	1 (AL)	1	3–4	0	0	10–13	4–5	0
Mimetus puritanus	6th instar adult ♀	3	1	0	1	1	52–59	25–33	0	1	0	1 (PM)	1	3–4	0	1	13–16	5	1
Mimetus puritanus	6th instar adult ♂	3	1	0	1	1	40–63	26–32	2	1	0	1 (PM)	1	3–4	0	0	10–15	3–6	0
Mimetus sp. A	Adult ♂	1	1	0	1	1	27	?, 17	2	1	0	1 (PM)	1	4	0	0	14, 13	5, 4	0

[a] Numbers are per spinneret. *Australomimetus*, *Ero*, and *Mimetus* data are from the same specimens examined in Townley and Tillinghast (2009). For rows containing data from one spider ($N = 1$), numbers of a given structure from the left and right of a spinneret pair are presented separately if the number per spinneret varied or could not be determined for one spinneret of the pair. For all other rows ($N \geq 2$), ranges of values are presented if variation was observed. See Townley and Tillinghast (2009) for data from juvenile *M. notius* and *M. puritanus*. Abbreviations: 1°, primary; 2°, secondary; Ac, aciniform silk glands; ALS, anterior lateral spinneret; Cyl, cylindrical silk glands; MaA, major ampullate silk glands; MiA, minor ampullate silk glands; MoPi, modified piriform silk glands; Pi, piriform silk glands; PLS, posterior lateral spinneret; PMS, posterior median spinneret.

[b] Position of 2° MiA tartipore given parenthetically relative to 2° MiA nubbin (adults) or 2° MiA spigot (juveniles); AL (anterolateral), AM (anteromedial), L (lateral), or PM (posteromedial) to 2° MiA nubbin/spigot.

[c] These two adult ♂ *P. sagittifer* are likewise designated 'adult ♂-1' and 'adult ♂-2' in Fig. 2 caption and Sect. 2.1.

[d] MoPi spigots in *Ero* differ in some respects from those of *Mimetus* and *P. sagittifer*. See Sects. 1 and 4.2.

from adult male and female *P. sagittifer* are presented in Figs. 2 and 3, respectively, and those from adult male, adult female, and penultimate instar female *Phobetinus* sp. PNG are shown in Figs. 4–6, respectively.

The following observations largely highlight characters that are variable among mimetines and thus apt to be most useful for improving our understanding of mimetine relationships.

3.1. Spinning apparatus features common to P. sagittifer and Phobetinus sp. PNG

3.1.1. Cylindrical silk gland (Cyl) spigots of females

Adult females of both species had a single Cyl spigot on each PMS (typical among araneoids) and on each PLS (not typical among araneoids, see Sect. 1) (Table 1) that were basically of the mimetine type; that is, very broad, with substantial bases and dome-shaped shafts (see Sect. 2.4) having large-diameter openings (Figs. 3D–F, and 5C, E). However, while their shafts were finely striated (Figs. 3E and 5E), they all lacked incisions. The penultimate instar female *Phobetinus* sp. PNG had the same complement of Cyl spigots as adult female mimetines (Table 1), but with less of a disparity in size relative to other spigot types and with narrower, less-rounded shafts having only small openings (Fig. 6B–D).

3.1.2. Occurrence of secondary (2°) minor ampullate silk glands (MiA) in males and females

The presence of functional 2° MiA in juvenile males and females was strongly indicated by the 2° MiA nubbin and 2° MiA tartipore on each PMS in adults (Figs. 2F, 3D, and 5B), and confirmed by the 2° MiA spigot and 2° MiA tartipore on each PMS in the penultimate instar female *Phobetinus* sp. PNG (Fig. 6B, C). Only the adult male *Phobetinus* sp. PNG differed by having no obvious 2° MiA nubbin on either PMS (Fig. 4D; Table 1). However, this does not appear to reflect an absence of 2° MiA while a juvenile, as this individual did have 2° MiA tartipores (which would serve no purpose without functioning 2° MiA in the preceding stadium), and the occurrence of nubbins can sometimes be variable (Townley and Tillinghast, 2003). Moreover, some 2° MiA nubbins that did form were very small (e.g., Fig. 3D) and thus only a short step from lacking discernible nubbins altogether. We therefore consider the two species equivalent in their possession of 2° MiA.

3.1.3. Posterior lateral spinneret (PLS) tartipore-accommodated (T-A) aciniform silk glands (Ac) in males and females

Ac tartipores were present on all PLS, demonstrating the presence, in both *Phobetinus* species, of T-A Ac that have spigots on the PLS. The only difference between species was that *P. sagittifer* had two Ac tartipores per PLS (Figs. 2G and 3F), while *Phobetinus* sp. PNG had one per PLS (Figs. 4E, F, 5C, D, and 6D) (Table 1). The location of the single Ac tartipore in *Phobetinus* sp. PNG was consistent with that of the more ectal of the two tartipores in *P. sagittifer*. As in all mimetids (and araneoids) examined to date, no Ac tartipores were observed on the PMS.

3.1.4. Potential vestiges of aggregate silk gland (Ag) or flagelliform silk gland (Fl) spigots

No Ag or Fl spigots were present on any specimen, nor were there any putative nubbins potentially representing phylogenetic vestiges of Ag/Fl spigots. However, in both species, in about the position on the PLS where Ag/Fl spigots occur in many araneoids, a putative sensillum containing a single raised-rim pore was present (Figs. 2G, 3F, and 4E, G). As in *Mimetus*, two raised-rim pores were also present on each PMS near the base of the 1° MiA spigot (Figs. 2F, 3D, 4D, and 6B) and several were on each MaA spinning field on the ALS (Figs. 2C, 3A, 4A, B, 5A, and 6A; examples from *Mimetus* in Fig. 1A, B, D), occupying positions and with a morphology comparable to mechanoreceptors (monitoring forces on spigots) described in the ctenid *Cupiennius* Simon, 1891 (Gorb and Barth, 1996; Barth, 2002).

3.1.5. Coluli

A subtriangular colulus with two serrate setae, and a tracheal spiracle a short distance (~40 μm) anterior to this, was common to males and females of both species (Figs. 2B and 6E).

3.2. Spinning apparatus features differing between P. sagittifer and Phobetinus sp. PNG: piriform silk gland (Pi) spigots in males

In both of the adult male *P. sagittifer* examined, two Pi spigots on each ALS were conspicuously different from the other spigots on the Pi spinning field. Their number, morphology, and location on the ALS largely matched those of MoPi spigots described in *Mimetus* (Townley and Tillinghast, 2009) and, thus, we likewise identified them as MoPi spigots (Table 1). The shafts of these spigots were wider and less tapered than those of the other Pi spigots (Fig. 2C, asterisks), with substantially larger-caliber openings (Fig. 2D, E, asterisks). For comparison, an ALS from an adult male *Mimetus puritanus* Chamberlin, 1923 is shown in Fig. 1B–D. Note that the MoPi spigots in *P. sagittifer* and *M. puritanus* were adjacent to and just anterior of the 2° MaA tartipore, separated from the typical Pi spigots by a fold in the cuticle (Figs. 1B–D and 2C–E, asterisks). A difference between these two genera was that there was in addition a fold or groove between the two MoPi spigots in *P. sagittifer* (Fig. 2C, E), while the cuticle between these two spigots in *Mimetus* was smooth (Fig. 1C, D). Also, the morphology of the MoPi spigot bases, not of substantial height in any case, differed between the two genera; those in *P. sagittifer* tending to be slightly sunken relative to the surrounding cuticle (Fig. 2C–E) (also seen in some other *Phobetinus* Pi spigots, e.g., Fig. 3A, B).

On each ALS of the adult male *Phobetinus* sp. PNG, there were, as in the *P. sagittifer* males, two Pi spigots just anterior of the 2° MaA tartipore. These did not, however, have noticeably wider shafts than the other Pi spigots (Fig. 4A, B, stars). Also, though the openings of the spigots in question, on both ALS, were at least partially obscured by secretion, a conspicuously larger caliber was not indicated (Fig. 4C, star). The shafts of these two Pi spigots were also a little further apart (Fig. 4A, B, stars) than those of the MoPi spigots in *P. sagittifer* (Fig. 2C, asterisks) or *M. puritanus* (Fig. 1B–D, asterisks). We therefore do not designate them MoPi spigots (Table 1).

The adult female *P. sagittifer* also had two Pi spigots per ALS in positions similar to those of the MoPi spigots of *P. sagittifer* males, though again more widely separated than the MoPi spigots (Fig. 3A–C, stars). Any differences between these Pi spigots, which presumably served non-T-A Pi, and the other spigots on the Pi spinning field, which presumably served T-A Pi, were marginal at most, the former having shafts that were perhaps less tapered and with modestly larger apertures (Fig. 3A–C, noting that the slightly damaged openings of these spigots in Fig. 3C may exaggerate differences in aperture diameters). Thus, as in *Mimetus*, unequivocal MoPi spigots were restricted to the adult male. The arrangement of the two presumed non-T-A Pi spigots was similar in the adult (Fig. 5A) and penultimate instar (Fig. 6A) female *Phobetinus* sp. PNG, with the more posterior of the two spigots adjacent to the anterior edge of the 2° MaA tartipore, though in the penultimate instar these two Pi spigots were especially widely separated.

3.3. Taxonomic illustrations

Given the paucity of studies on *Phobetinus*, not surprisingly there are few images of the genus in the literature. Included here

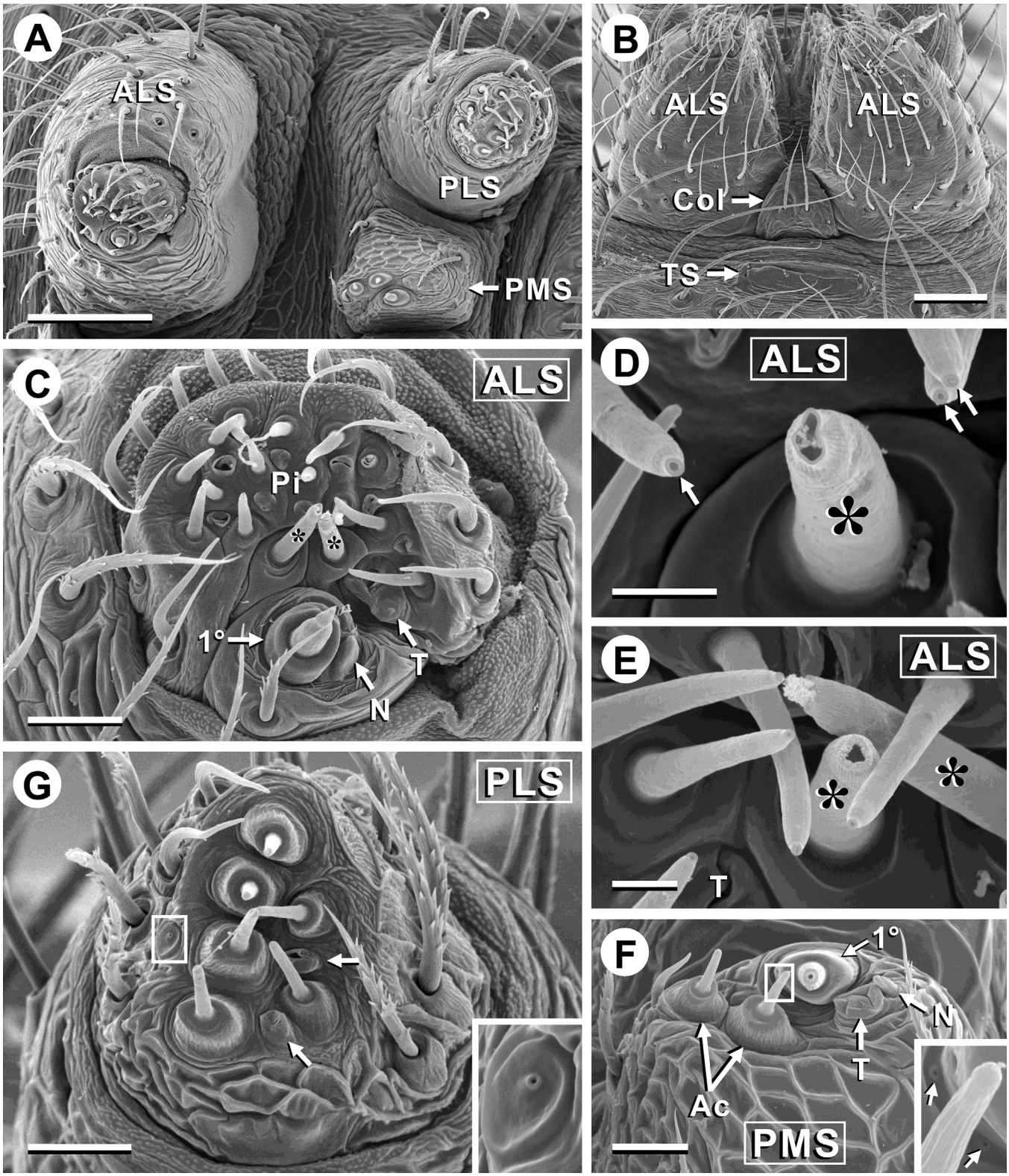

Fig. 2. Spinnerets of adult male *Phobetinus sagittifer*. A. Spinnerets, left side of abdomen, adult ♂-2. B. Anterior view of ALS pair, adult ♂-2, showing colulus (Col) and tracheal spiracle (TS). C. Left ALS, adult ♂-2, MoPi spigots indicated by asterisks. D. Left ALS, adult ♂-1, close-up of anterior MoPi spigot (asterisk) compared to three T-A Pi spigots (arrows). E. Right ALS, adult ♂-1, close-up of MoPi spigots (asterisks) and five T-A Pi spigots; opening of anterior MoPi spigot obscured by debris, but large opening of posterior MoPi spigot apparent. F. Right PMS, adult ♂-1, boxed area magnified in inset, showing two raised-rim pores (arrows). G. Left PLS, adult ♂-2, all six spigots serve Ac; arrows indicate two Ac tartipores; boxed area contains a raised-rim pore sensillum, magnified in inset. Anterior at left, mesal at bottom in (A, C, D, G); anterior right, mesal bottom in (E); anterior left, mesal top in (F). Scale bars: A, B 50 μm; C, F, G 10 μm; D, E 2 μm. 1°, 1° MaA spigot (on ALS) or 1° MiA spigot (on PMS); Ac, Ac spigots; N, 2° MaA nubbin (on ALS) or 2° MiA nubbin (on PMS); Pi, Pi spinning field; T, 2° MaA tartipore (on ALS) or 2° MiA tartipore (on PMS).

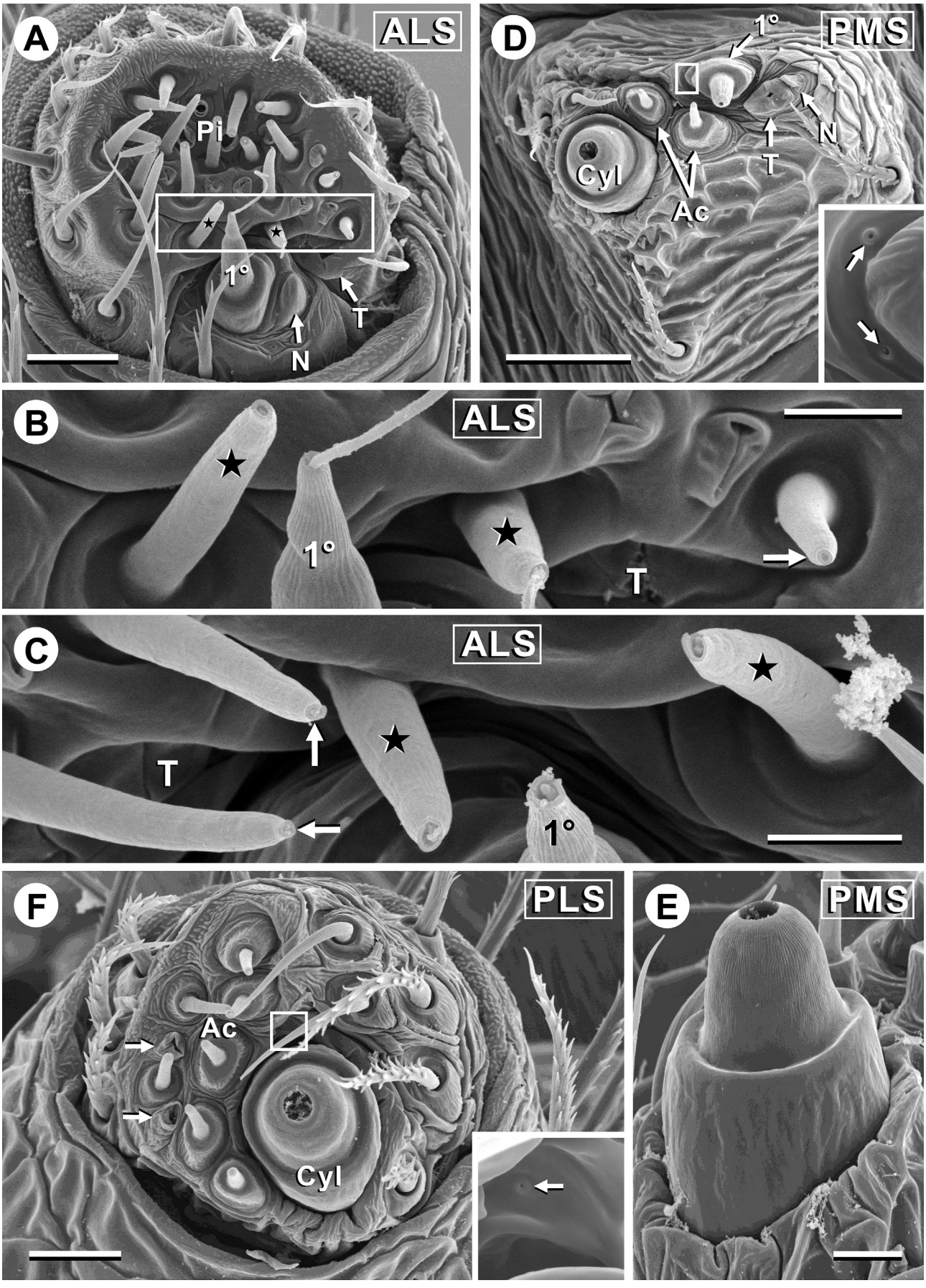
A
ALS
Pi
1°
T
N
D
PMS
1°
N
T
Cyl
Ac
B
ALS
1°
T
C
ALS
T
1°
F
PLS
Ac
Cyl
E
PMS

are representations of *P. sagittifer* structures to further aid identification. Drawings and micrographs of male pedipalps are shown in Fig. 7, which includes alternative drawings of the lectotype illustrated in Brignoli (1972), MNHN 16304 (Fig. 7A–C). Fig. 8 presents habitus and epigynum drawings from a female. In Fig. 9 the male pedipalp of *P. sagittifer* is compared with palps from representatives of *Australomimetus*, *Ero*, and *Mimetus*.

4. Discussion

The Cyl spigots of *Phobetinus* provided support for placement of this genus in the subfamily Mimetinae (Sect. 4.1). Though equivocal, overall the suite of spinneret features observed in *Phobetinus* indicated degrees of relatedness to the three previously examined mimetine genera in the order (high to low) *Mimetus–Australomimetus–Ero* (Sect. 4.1–4.4).

One feature found to be unique to the spinning fields of *Phobetinus* was that the position taken by *Mimetus*-type MoPi spigots in adult male *P. sagittifer* was essentially the same as that taken by presumed non-T-A Pi spigots in adult and penultimate instar females (cf. Figs. 2C, 3A, 5A, and 6A). In *Mimetus*, in contrast, non-T-A Pi spigots in adult females and juveniles have been observed in a position ectal to that taken by the adult male's MoPi spigots (Sect. 4.2) (cf. Fig. 1A, B; see also Griswold et al., 2005; Townley and Tillinghast, 2009).

4.1. Cylindrical silk gland (Cyl) spigots in females

Two synapomorphies of the subfamily Mimetinae have been proposed (see Sect. 1), both of which were exhibited by both *Phobetinus* species:

1) enlarged Cyl spigots with prominent bases, dome-shaped shafts, and wide openings (Platnick and Shadab, 1993).
2) a single Cyl spigot (as opposed to two) on each PLS (e.g., Figs. 3F and 5C).

The absence of incisions (grooves) on the shafts of *Phobetinus* Cyl spigots (Figs. 3E and 5E) makes them more similar to Cyl spigots of *Australomimetus*, which also lack incisions (Fig. 1E) (Harms and Harvey, 2009a, b; Townley and Tillinghast, 2009), than to Cyl spigots of *Ero* and *Mimetus*, which generally have incisions (Fig. 1F, G) (Platnick and Shadab, 1993; Schütt, 2000; Griswold et al., 2005; Townley and Tillinghast, 2009). If the plesiomorphic state is for incising to be absent (Platnick and Shadab, 1993; Harms and Harvey, 2009b) and if *Phobetinus* is most closely related to *Mimetus* (see Sect. 4.2–4.5), then the occurrence of shaft incising in *Mimetus* and *Ero* may well be an instance of parallelism. We note that while Cyl spigots in *Ero* and *Mimetus* can sometimes be strikingly grooved (Fig. 1F), in some species the range of variation extends to virtually no incising (Fig. 1G, inset). Any selective advantage of shaft incising remains to be determined.

4.2. Modified piriform silk gland (MoPi) spigots in males

Perhaps the strongest indication of close affinity between *Phobetinus* and *Mimetus* were the MoPi spigots of adult male *P. sagittifer* that occupied positions on each ALS and had a morphology similar to MoPi spigots of *Mimetus* (cf. Figs. 1B–D, 2C–E) (Townley and Tillinghast, 2009). These differed from the 'subtle' MoPi spigots of adult male *Ero tuberculata* (De Geer, 1778) and *E. aphana*, which are not positioned adjacent to the 2° MaA tartipore and not as easily distinguished or set apart from surrounding T-A Pi (see Sect. 1) (Fig. 14C, D and 15A–C in Townley and Tillinghast, 2009). The function of the products of MoPi is unknown. Their occurrence, restricted to adult males, suggests a role in reproduction. The following paragraphs consider how MoPi relate to other Pi.

By examining spinnerets on successive exoskeletons from the same individual (as in Fig. 1A, B), it has been determined in *M. notius, M. puritanus*, and the araneid *Araneus cavaticus* (Keyserling, 1881) that there are two non-T-A Pi spigots per ALS, at least on first through penultimate instars of both sexes (Townley and Tillinghast, 2009). They may likewise be present in adults, but as these determinations have been made by counting and matching positions of spigots in one stadium with tartipores in the following stadium, this is not a certainty since adults do not molt and, thus, there is no subsequent exoskeleton on which to examine tartipores. Given that possession of two pairs of non-T-A Pi spigots applies to an araneid as well as to *Mimetus*, it seems likely that it also applies to *Phobetinus*. This presumption, while not definitively proven, was upheld by comparing the number of Pi spigots in the penultimate instar *Phobetinus* sp. PNG (8–9/ALS) with the number of Pi tartipores in adults of the same species (6–7/ALS) (Table 1).

Since non-T-A silk glands have the potential to be used in every stadium (see Sect. 2.4), it has been suggested that the same two pairs of non-T-A Pi may function throughout ontogeny, re-modeled at each proecdysis (Townley and Tillinghast, 2009). If so, they are like 1° MaA and 1° MiA, which are also non-T-A silk glands (Townley et al., 1993; Townley and Tillinghast, 2003). Going a step further, it may be that MoPi in *Mimetus* and *P. sagittifer* are the same entities as the non-T-A Pi first used in the first stadium, just modified more radically during the final proecdysis, with unique spigots being an external manifestation of this change (Townley and Tillinghast, 2009). This would suggest that adult male MoPi are homologous with non-T-A Pi not only in other mimetids, but also in other araneoids.

This hypothesis (Hypothesis **1**), whereby MoPi develop from pre-existing non-T-A Pi that have been in use since the first stadium, is opposed to Hypothesis **2** whereby MoPi develop *de novo* in penultimate instar males.

In support of Hypothesis **2** is 1) the precedent provided by presumed *de novo* increases in numbers of certain silk glands that occur throughout ontogeny (e.g., T-A Pi and non-T-A Ac, see Figs. 5, 8, and 9 and Table 3 in Townley and Tillinghast, 2009), and 2) the absence, in adult female and juvenile *Mimetus* (Fig. 1A; also Figs. 4E, 5, 6B, and 13A in Townley and Tillinghast, 2009), of Pi spigots that occupy the site taken by MoPi spigots in adult male *Mimetus* (i.e., next to the anterior end of the 2° MaA tartipore) (Fig. 1B, D, asterisks; also Fig. 3A, C, and 4A, B in Townley and Tillinghast, 2009).

Hypothesis **1** is supported, in *Mimetus*, 1) by agreement in the number of MoPi and non-T-A Pi (two pairs), 2) by similar (though not identical) positioning of MoPi and non-T-A Pi spigots on the mesal edge of the Pi spinning field, and 3) by the precedent provided by non-T-A silk glands (e.g., 1° MaA, 1° MiA (Townley et al.,

Fig. 3. Spinnerets of adult female *Phobetinus sagittifer*. A. Left ALS, boxed area contains non-T-A Pi spigots (stars). B. Boxed area from (A), magnified. C. Right ALS, close-up of non-T-A Pi spigots (stars). Arrows in (B–C) point to T-A Pi spigots. D. Right PMS, boxed area magnified in inset, showing two raised-rim pores (arrows). E. Right PMS, close-up of Cyl spigot. F. Right PLS, Ac spinning field (Ac) contains seven spigots and two tartipores (arrows); boxed area contains a raised-rim pore sensillum, magnified (and from more tilted perspective) in inset (arrow to pore). Anterior at left, mesal at bottom in (A, B); anterior right, mesal bottom in (C, F); anterior left, mesal top in (D, E). Scale bars: D 20 μm; A, F 10 μm; E 5 μm; B, C 3 μm. 1°, 1° MaA spigot (on ALS) or 1° MiA spigot (on PMS); Ac, Ac spigots/spinning field; Cyl, Cyl spigot; N, 2° MaA nubbin (on ALS) or 2° MiA nubbin (on PMS); Pi, Pi spinning field; T, 2° MaA tartipore (on ALS) or 2° MiA tartipore (on PMS).

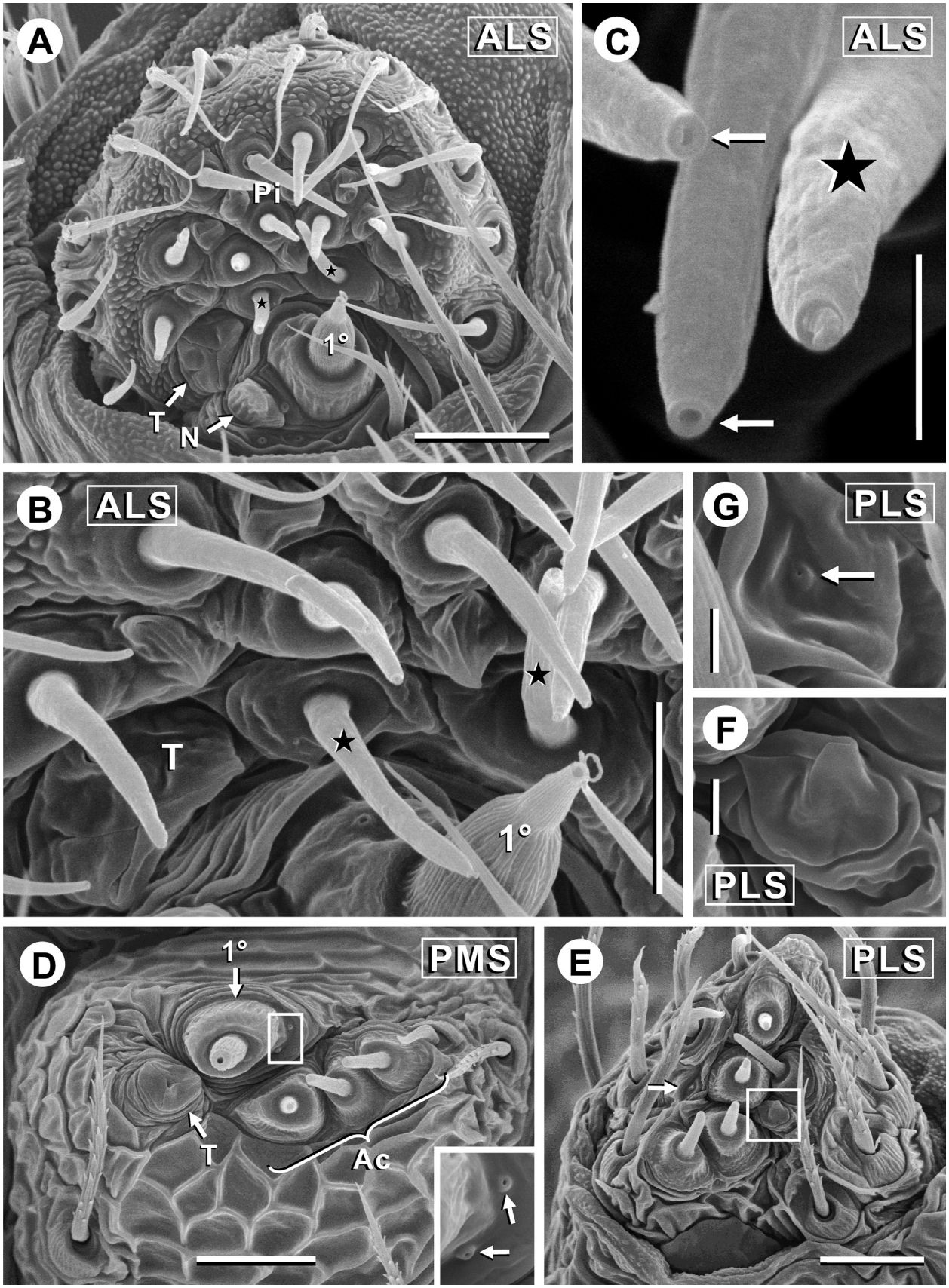

Fig. 4. Spinnerets of adult male *Phobetinus* sp. PNG. A. Right ALS, non-T-A Pi spigots indicated by stars. B. Same spinneret, showing no clear morphological differences between non-T-A Pi spigots (stars) and T-A Pi spigots (all other spigots in frame, apart from 1° MaA spigot (1°)). C. Left ALS, comparison of shafts of one non-T-A Pi spigot (star) and two T-A Pi spigots (arrows): no clear difference. D. Left PMS, boxed area magnified in inset, showing two raised-rim pores (arrows). Note apparent absence of 2° MiA nubbin. E. Left PLS, all five spigots serve Ac; single Ac tartipore in boxed area; location of raised-rim pore sensillum indicated by arrow. F. Ac tartipore from boxed area in (E), magnified. G. Sensillum on right PLS; arrow to raised-rim pore. Anterior at right, mesal at bottom in (A, B, G); anterior left, mesal bottom in (C, E, F); anterior right, mesal top in (D). Scale bars: A, D, E 10 μm; B 5 μm; C, F, G 1 μm. 1°, 1° MaA spigot (on ALS) or 1° MiA spigot (on PMS); Ac, Ac spinning field; N, 2° MaA nubbin; Pi, Pi spinning field; T, 2° MaA tartipore (on ALS) or 2° MiA tartipore (on PMS).

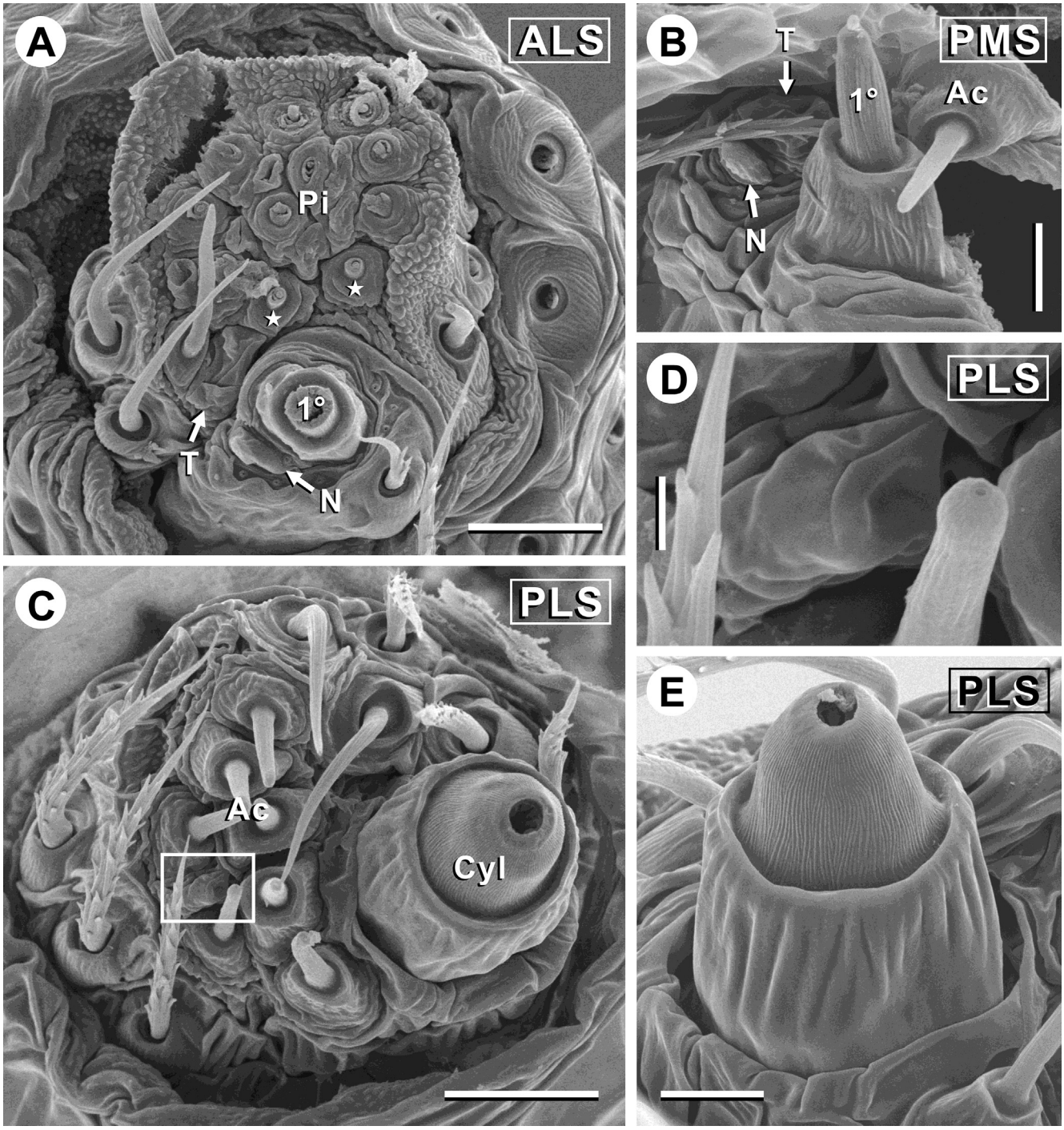

Fig. 5. Spinnerets of adult female *Phobetinus* sp. PNG. A. Right ALS, non-T-A Pi spigots indicated by stars (shafts broken off, as with all but one Pi spigot). B. Portion of right PMS, contorted and torn, but with 2° MiA nubbin (N) and tartipore (T) clearly present. C. Right PLS, Ac spinning field (Ac) contains seven spigots and one tartipore (boxed area). D. Ac tartipore from boxed area in (C), magnified. E. Left PLS, close-up of Cyl spigot. Anterior at right, mesal at bottom in (A–D); anterior left, mesal bottom in (E). Scale bars: A, C 10 μm; B, E 5 μm; D 1 μm. 1°, 1° MaA spigot (on ALS) or 1° MiA spigot (on PMS); Ac, Ac spigot/spinning field; Cyl, Cyl spigot; N, 2° MaA nubbin (on ALS) or 2° MiA nubbin (on PMS); Pi, Pi spinning field; T, 2° MaA tartipore (on ALS) or 2° MiA tartipore (on PMS).

1993)) that function from the first stadium through adulthood. *Phobetinus* provided additional support for Hypothesis **1** by at least partially negating the second argument given in support of Hypothesis **2**. In *P. sagittifer*, MoPi spigots of adult males sat adjacent to the 2° MaA tartipore as in *Mimetus* (Fig. 2C, E, asterisks), but, unlike *Mimetus*, there were also Pi spigots, presumably non-T-A, in the adult female that occupied essentially the same position (Fig. 3A–C, stars). This positional similarity likewise applied to presumed non-T-A Pi spigots in juvenile (Fig. 6A, stars) and adult (Figs. 4A, B, and 5A, stars) *Phobetinus* sp. PNG. It is true that positions were not identical: the two non-T-A Pi spigots on an ALS (Figs. 3–6, stars) were more separated than the two MoPi spigots in *P. sagittifer* males (Fig. 2C, asterisks), but at least the more posterior of the two non-T-A Pi spigots was adjacent to the 2° MaA tartipore. Assuming MoPi originate in the same way in *Mimetus* and *P. sagittifer*, this positional correspondence in

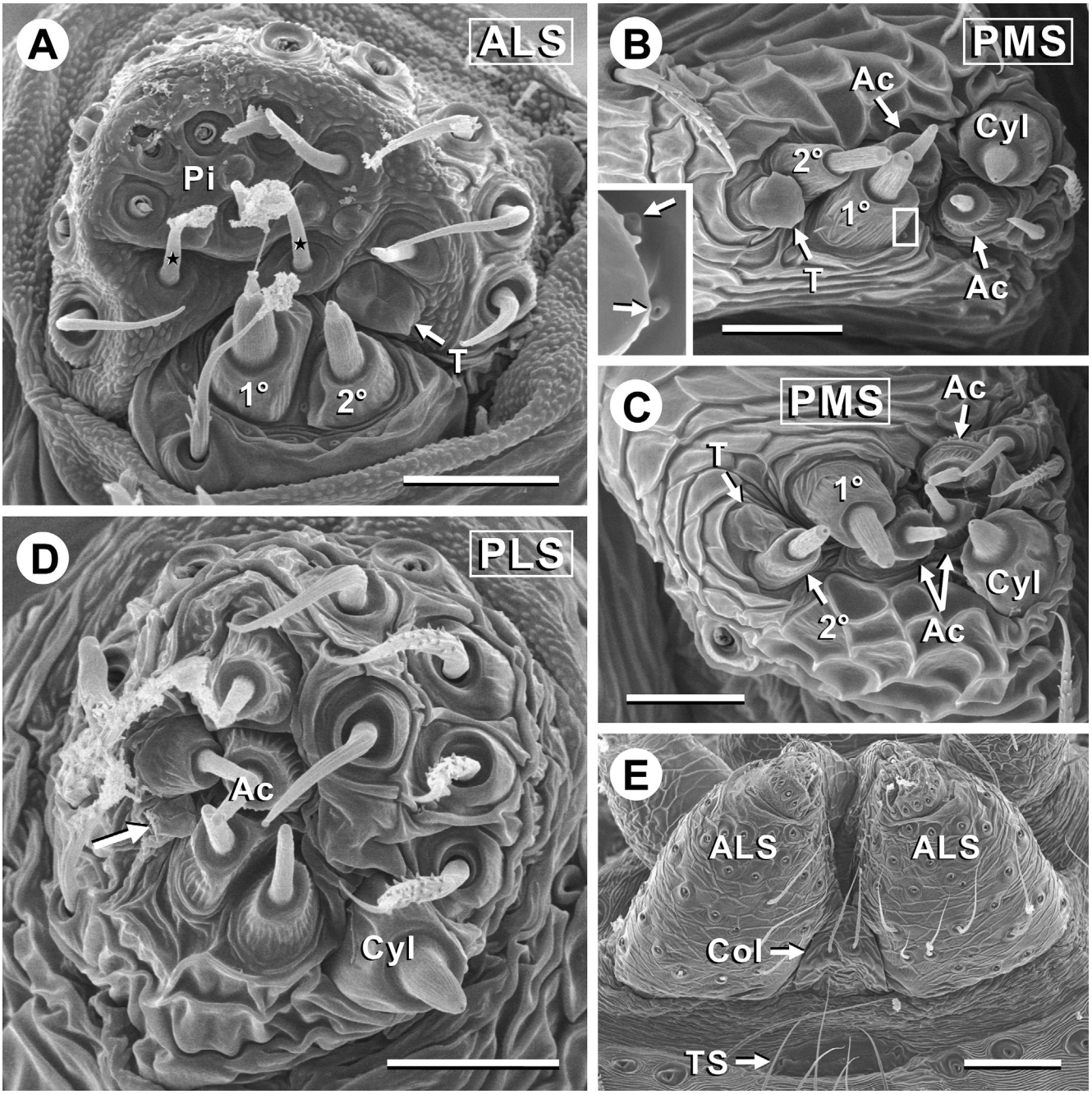

Fig. 6. Spinnerets of penultimate instar female *Phobetinus* sp. PNG. A. Left ALS, non-T-A Pi spigots indicated by stars. B. Right PMS, boxed area magnified (and from more anterior perspective) in inset, showing two raised-rim pores (arrows). C. Left PMS. D. Right PLS, Ac spinning field (Ac) contains five spigots and one tartipore (arrow). E. Anterior view of ALS pair showing colulus (Col) and tracheal spiracle (TS). Anterior at left, mesal at bottom in (A); anterior right, mesal bottom in (B, D); anterior right, mesal top in (C). Scale bars: E 50 μm; A–D 10 μm. 1°, 1° MaA spigot (on ALS) or 1° MiA spigot (on PMS); 2°, 2° MaA spigot (on ALS) or 2° MiA spigot (on PMS); Ac, Ac spigot/spinning field; Cyl, Cyl spigot; Pi, Pi spinning field; T, 2° MaA tartipore (on ALS) or 2° MiA tartipore (on PMS).

Phobetinus, which suggested homology between MoPi and non-T-A Pi, appeared to favor Hypothesis **1**.

A recent observation made in *Mimetus* also appeared to support Hypothesis **1**. Fig. 1B shows the right ALS from an adult male *M. puritanus* and Fig. 1A shows the same spinneret on the final exuvium shed by the same individual. During the final proecdysis, the adult cuticle (Fig. 1B) formed beneath the penultimate instar cuticle (Fig. 1A), with tartipores in the adult cuticle encircling, and thereby accommodating, ducts emptying on the penultimate instar's T-A Pi spigots and 2° MaA spigot. By comparing the Pi spigots in Fig. 1A to the Pi tartipores in Fig. 1B, we identified the two non-T-A Pi spigots in the penultimate instar (Fig. 1A, unlabeled arrows). Hypothesis **1** proposes that the Pi emptying on these non-T-A Pi spigots were re-modeled during the final proecdysis, with one change being that their ducts detached from the non-T-A Pi spigots indicated in Fig. 1A and then connected to the MoPi spigots in Fig. 1B. If so, there would be no need for non-T-A Pi spigots to form on the adult cuticle in the position where they occurred on the penultimate instar cuticle (since MoPi spigot position is mesal to non-T-A Pi spigot position), creating the potential for a vacancy to exist on the adult cuticle. Indeed, consistent with this predicted absence of non-T-A Pi spigots, there is a bare patch of cuticle on the

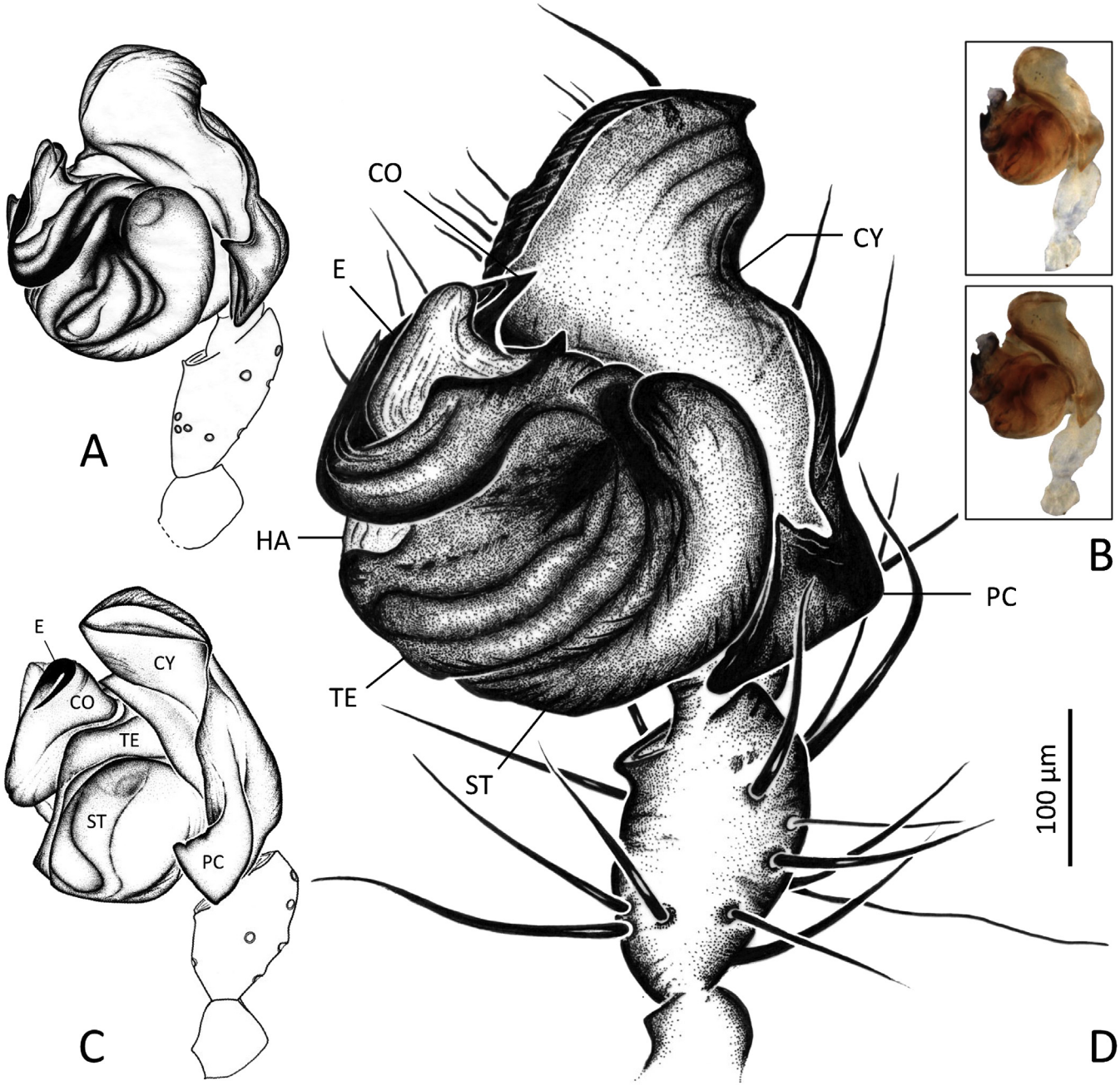

Fig. 7. Illustrated male pedipalps of *Phobetinus sagittifer*. A–C. Reconstruction of lectotype (MNHN Inventory AR14618, Object 16304). A. Frontolateral view. B. Automontage images of frontolateral (upper) and lateral (lower) views. C. Lateral view. D. Male deposited at MHNG, frontolateral view. CO, conductor; CY, cymbium; E, embolus; HA, haematodocha; PC, paracymbium; ST, subtegulum; TE, tegulum.

adult ALS just above the MoPi spigots in Fig. 1B (enlarged in Fig. 1C, arrow), corresponding reasonably well to the position occupied by the non-T-A Pi spigots in the penultimate instar. This bare patch has not been as obvious in previous male *Mimetus* preparations and was perhaps apparent in this preparation because of especially well distended ALS.

In light of these recent observations from *Phobetinus* and *Mimetus*, which weaken one of the arguments in support of Hypothesis **2** and are consistent with a prediction of Hypothesis **1**, respectively, we think the evidence currently available favors Hypothesis **1**.

By this interpretation, the absence of MoPi spigots in the adult male *Phobetinus* sp. PNG does not signal the absence of Pi that are one-to-one homologous to MoPi, only that modifications made during the final proecdysis to the homologs (non-T-A Pi) in males of this species are less extreme, at least with regard to spigot morphology, than those made to non-T-A Pi in male *Mimetus* and *P. sagittifer*. This interpretation would also mean that MoPi in *Mimetus*/*P. sagittifer* and the aforementioned 'subtle' MoPi described in two (of 5) *Ero* species are indeed homologs (Townley and Tillinghast, 2009), both modified from non-T-A Pi. We note that *Ero*-like subtle MoPi spigots have also recently been observed in adult males of *Australomimetus sydneyensis* Heimer 1986 (D. Harms and M. Townley, unpublished observations).

4.3. Secondary (2°) minor ampullate silk glands (MiA)

As demonstrated by the presence of a 2° MiA tartipore and 2° MiA spigot (juveniles) or nubbin (adults) on each PMS, 2° MiA occur

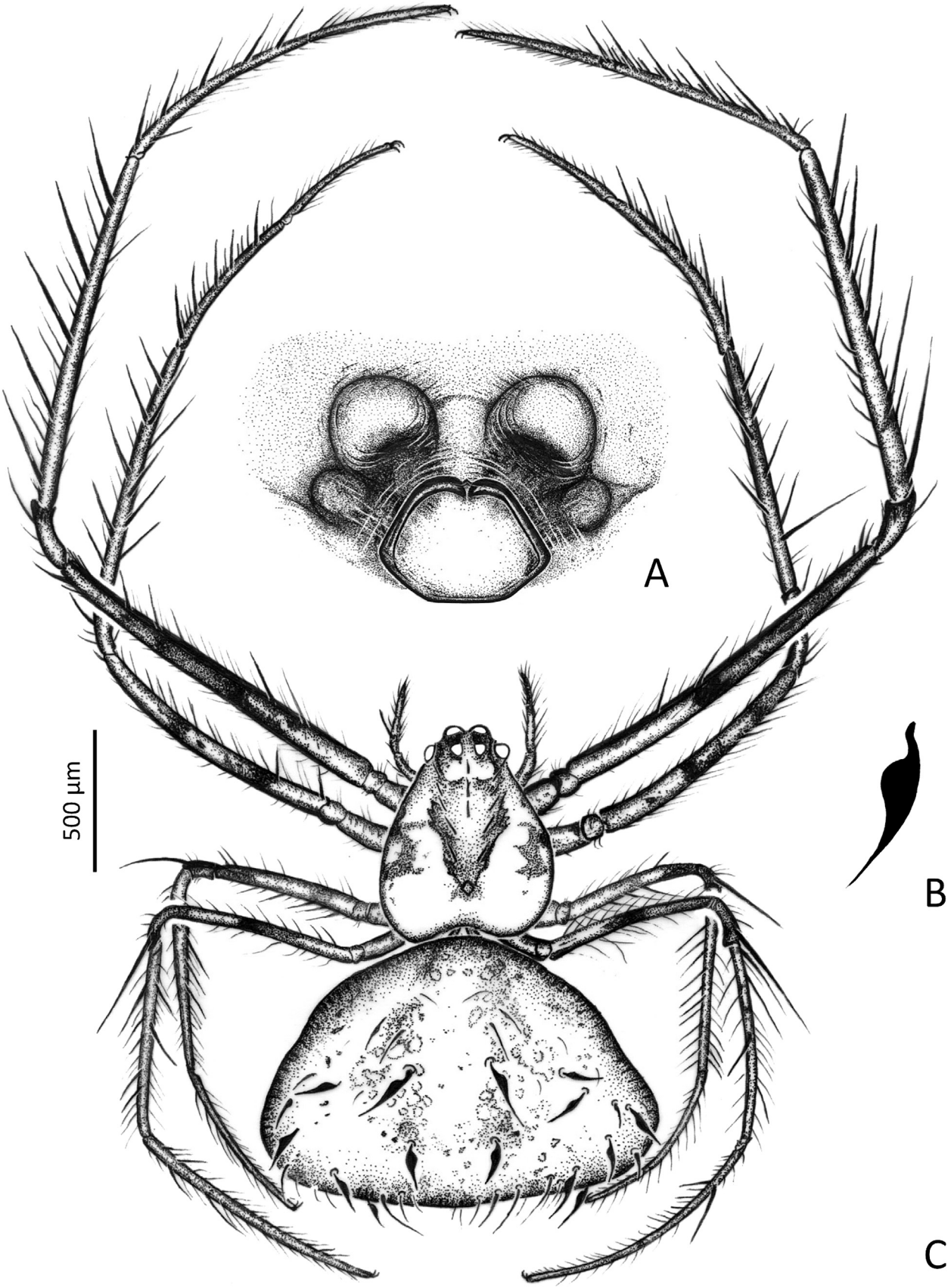

Fig. 8. Illustrated female of *Phobetinus sagittifer* (deposited at MHNG). A. Epigynum in ventral view. Note the large posterior genital opening. B. Detail of abdominal seta in lateral view. C. Habitus in dorsal view.

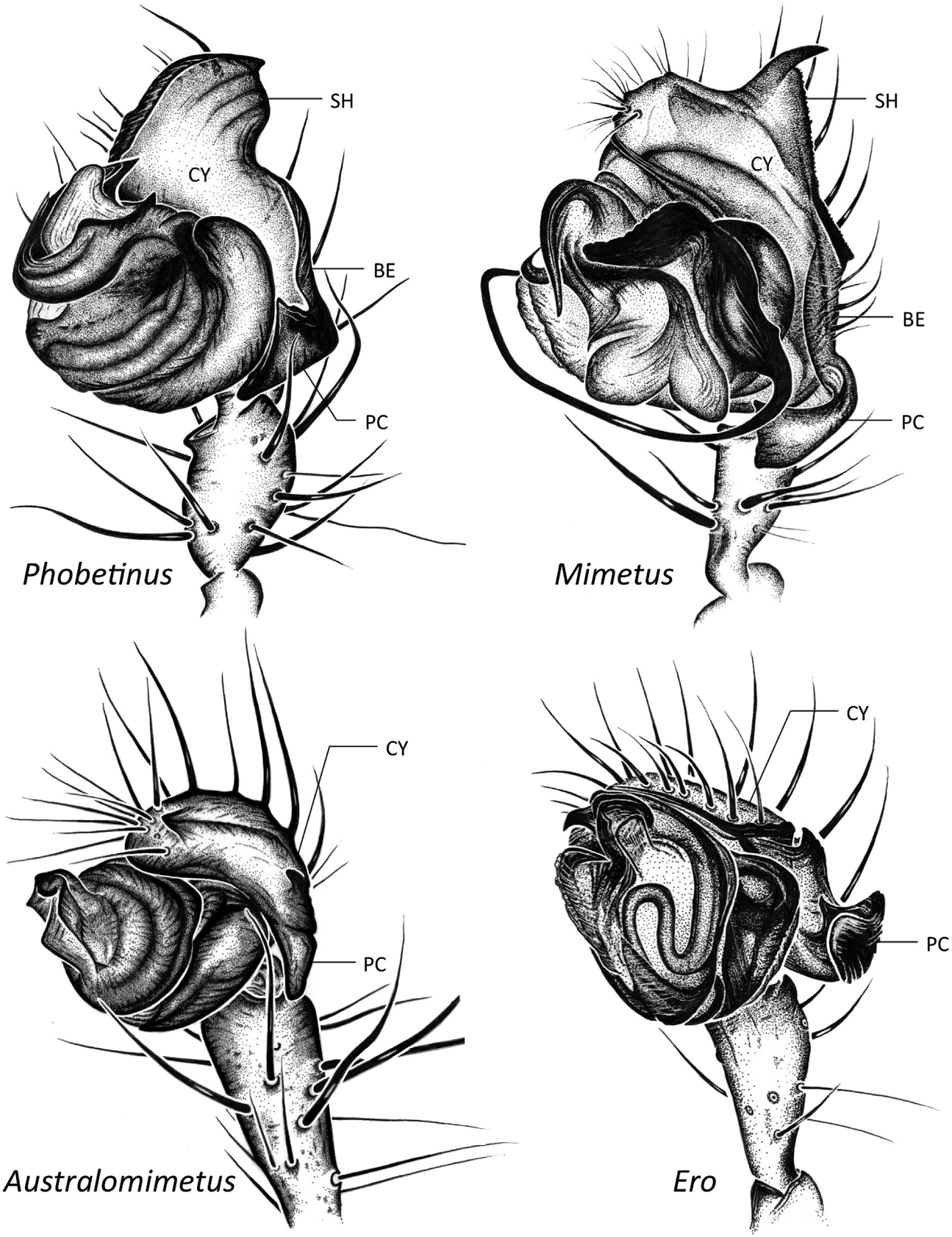

Fig. 9. Illustrated male pedipalps of four exemplar mimetine species in frontolateral view: *Phobetinus sagittifer* from Sri Lanka, type species of the genus; *Mimetus syllepsicus* from USA, type species of the genus (modified from Harms and Harvey, 2009b); *Australomimetus* sp. from Indonesia, representative of the genus; *Ero aphana* from Western Australia, representative of the genus. Note the peculiar similarities between the type species of *Mimetus* and *Phobetinus*, such as the enlarged and distally extended cymbium (CY) that forms a pointed "shovel-like appendage" (Heimer, 1986) (SH) and the subtriangular paracymbium (PC). In contrast, the pedipalps of *Australomimetus* and *Ero* have a simple cymbium without distal and retrolateral extensions, and a paracymbium that is not subtriangular. BE, basal extension of cymbium.

in juveniles of all five *Mimetus* species examined to date by SEM, including the type species *M. syllepsicus* (Platnick and Shadab, 1993; Griswold et al., 2005; Townley and Tillinghast, 2009). This is the plesiomorphic state (Forster et al., 1990; Scharff and Coddington, 1997). They are also apparently present in four of five *Australomimetus* species, including the type species *A. maculosus* (Rainbow, 1904) (Harms and Harvey, 2009b; Townley and Tillinghast, 2009), but in only two of seven *Ero* species, and not the type species *E. tuberculata* (Platnick and Shadab, 1993; Townley and Tillinghast, 2009). By itself, the presence of 2° MiA in both examined *Phobetinus* species (Figs. 2F, 3D, 4D, 5B, and 6B, C) does not preclude an especially close relationship between *Phobetinus* and *Ero*, but it does seem least likely.

4.4. Posterior lateral spinneret (PLS) tartipore-accommodated (T-A) aciniform silk glands (Ac)

The presence of tartipores in the Ac spinning field on the PLS testifies to the presence of PLS T-A Ac, which is the presumed plesiomorphic condition. They have been observed in all examined *Mimetus* (5 species), but in no *Australomimetus* (5 species) or *Ero* (7 species) (Platnick and Shadab, 1993; Schütt, 2000; Griswold et al., 2005; Harms and Harvey, 2009b; Townley and Tillinghast, 2009). Their occurrence in both *Phobetinus* species (Figs. 2G, 3F, 4E, F, 5C, D, and 6D) lends support to an especially close affinity between *Phobetinus* and *Mimetus*. In *Mimetus*, non-T-A Ac spigots form a line along the anterior border of the Ac spinning field, with the T-A Ac spigots posterior to these (Fig. 1G; see also Figs. 8 and 9 in Townley and Tillinghast, 2009). All indications are that the same is true in *Phobetinus*. For example, in the penultimate instar *Phobetinus* sp. PNG (Fig. 6D), a line of four apparently non-T-A Ac spigots was observed anterior of a single T-A Ac spigot (directly above the only Ac tartipore in Fig. 6D). Had this individual molted to maturity, we would have expected the single T-A Ac to have left a single Ac tartipore in the adult cuticle, posterior to the line of non-T-A Ac spigots, exactly as seen in the examined adults of this species (Figs. 4E and 5C).

4.5. Genital morphology

Though our focus here is on spinning field characteristics, the overriding goal is a better understanding of relationships within the Mimetidae. Toward that end, we note that phylogenetic affinities between *Phobetinus* and *Mimetus* are also apparent by virtue of genital morphology, in particular between adult males (Fig. 9). The type species of both genera share a peculiar arrangement of the cymbium that is greatly enlarged and exceeds the bulb and tegular apophyses both distally and retrolaterally. The distal extension ("shovel-like appendage" in Heimer, 1986) is pointed and heavily sclerotized. There is also a basal sclerotization on the retromargin of the cymbium that is bent toward the tegulum and serves as an insertion point for the paracymbium. The paracymbium itself is often subtriangular, distally broadened, and integrated into the cymbium so that the junction between paracymbium and cymbium is confluent. These features are entirely absent in *Australomimetus* and *Ero*, which often have a simple cymbium without distal and retrolateral processes, and a paracymbium that is rounded distally.

Differences in genital morphology figured prominently in a cladistic analysis that was concerned primarily with relationships among species of *Australomimetus* (Harms and Harvey, 2009b), but which included as outgroup species the type species of *Mimetus*, *Phobetinus*, and *Ero*, and a second *Mimetus* species. Of 87 characters in the data matrix, 62 were derived from genital morphology, only one from spinning field morphology (shape of Cyl spigots). The resulting cladogram hypothesized a sister-group relationship between *Phobetinus* and *Mimetus* that was strongly supported by three unambiguous characters derived from genital morphology and placed *Australomimetus* more distant, consistent with our overall impressions from spinning field features.

4.6. Numbers of piriform silk gland (Pi) and aciniform silk gland (Ac) spigots

From the mimetine data currently available (Table 1), *Phobetinus* appeared least like *Mimetus* in terms of numbers of Pi and Ac spigots (especially those on the PLS), with *Mimetus* having greater numbers of both. This may be a consequence of *Mimetus* maturing at later stadia than other mimetines, but available evidence suggests otherwise. *M. notius* and *M. puritanus* can reach maturity as fifth or sixth instars (Townley and Tillinghast, 2009). Fifth instar adults have a 2° MiA tartipore that occurs anterolateral to the 2° MiA nubbin, while in sixth instar adults it is posteromedial (Table 1). If *Phobetinus* are like *Mimetus* in having this tartipore placed anterolaterally in odd-numbered instars and posteromedially in even-numbered instars (not yet determined), then the penultimate instar female *Phobetinus* sp. PNG we examined, with its posteromedially positioned tartipore (Table 1), was presumably either a second or fourth instar. The latter was indicated by the presence of Cyl spigots, which in *Mimetus* at least were first seen in third instars, and especially by the number of Pi tartipores (4/ALS), which would likely be two per ALS in a second instar, as in *Mimetus* (Townley and Tillinghast, 2009). If this is correct, then the adult *Phobetinus* we examined were, like many adult *Mimetus*, fifth instars.

A more likely explanation for differences in numbers of Pi and Ac spigots relates to differences in body size, with the more capacious abdomens of examined *Mimetus* able to accommodate larger numbers of silk glands than the smaller *Phobetinus*. In any case, the phylogenetic significance of these differences in Pi/Ac numbers is questionable, especially given the ranges sometimes seen within a genus (Table 1).

4.7. Triad vestiges

On each PLS of *Phobetinus*, the only possible vestige of an ancestral Ag-Fl triad (three spigots: two Ag, one Fl) that we observed was a single round to oval patch of cuticle containing one raised-rim pore that occurred in a position consistent with an araneoid triad (Figs. 2G, 3F, and 4E, G). These have also been seen in *Mimetus*, *Australomimetus*, and *Ero* (rarely, but significantly, a second pore was present in *M. puritanus*) (Townley and Tillinghast, 2009). Superficially, these have resembled sensilla associated with MaA spigots (e.g., Figs. 1D, 4A, 5A, and 6A) that were found by Gorb and Barth (1996) to have a mechanosensory function. Comparable sensilla may also be associated with 1° MiA spigots as two raised-rim pores occur adjacent to each 1° MiA spigot (Figs. 2F, 3D, 4D, and 6B; see also Townley and Tillinghast, 2009). For ease of discussion we will tentatively refer to all such raised-rim pore structures as sensilla, though, for those on the PLS and PMS, this remains to be established and other functions may be envisioned (e.g., glandular secretion). If a sensory function is correct, however, then sensilla resembling those on the PLS of mimetines are often associated with specific spigots, raising the possibility that the mimetine PLS sensillum was likewise associated ancestrally with specific spigots; namely, Ag-Fl spigots or their homologs. That raised-rim pore sensilla are indeed associated with Ag-Fl spigots has been indicated in *Araneus*, where three such pores per triad have been seen (Fig. 10D in Townley and Tillinghast, 2009), and in linyphiids, where one or two pores have been observed near each Fl spigot in species exhibiting loss of Ag spigots (Schütt, 1995). In

another araneid, *Cyrtophora*, which build webs lacking sticky spirals, the Ag-Fl triad has been lost, but its ancestral position is still occupied by two (occasionally one) raised-rim pore sensilla (Fig. 11a, b in Peters, 1993).

In both *Cyrtophora* (Peters, 1993) and *Mimetus* (Townley and Tillinghast, 2009), a protuberance occasionally develops adjacent to the PLS raised-rim pore sensillum. This has been interpreted as a possible phylogenetic vestige of a spigot (i.e., a phylogenetic nubbin). If so, in *Cyrtophora* there would be little doubt that such a nubbin represents either a Fl or Ag spigot present in an orb-web-building ancestor (Peters, 1993), and, though less certain, the same could be true of the *Mimetus* nubbin. In that case, the PLS sensillum in *Phobetinus* would indeed be a vestige of an Ag-Fl triad. Given that a protuberance on the PLS has only been observed in a minority of *M. notius*, all juveniles (Townley and Tillinghast, 2009), the absence of this protuberance in our six *Phobetinus* specimens, only one juvenile, was not surprising.

Acknowledgments

This research was supported by an Endeavour International Postgraduate Research Scholarship (EIPRS) and a UPAIS top-up scholarship of the University of Western Australia to DH. SPB was funded by a fellowship from the Alexander von Humboldt Foundation and the Institute of Fundamental Studies. We thank the Department of Wildlife Conservation and the Department of Forest Conservation of Sri Lanka for facilitating fieldwork in Sri Lanka. Ingi Agnarsson (University of Vermont) kindly provided the *Phobetinus* sp. PNG from Papua New Guinea for which we are very grateful. Many thanks also to Christine Rollard and Mark Judson (MNHN) for the loan of the *P. sagittifer* lectotypes, to Norman Platnick (AMNH), Jason Dunlop (ZMB) and Peter Schwendinger (MHNG) for the loan of other mimetine specimens used for illustrations, to Nancy Cherim (UNH) for once again facilitating use of the SEM, to Namal Atukorala, Sudesh Batuwita, and Harshini Sandamali (all of IFS) for assistance in the field in Sri Lanka, to Matjaž Kuntner (Slovenian Academy of Sciences and Arts) for collecting the male *Australomimetus* in Indonesia, and to Jörg Wunderlich (Hirschberg, Germany) for access to his private collection.

References

Barth, F.G., 2002. A Spider's World: Senses and Behavior (M.A. Biederman-Thorson, Trans.). Springer, Berlin.

Blackledge, T.A., Scharff, N., Coddington, J.A., Szüts, T., Wenzel, J.W., Hayashi, C.Y., Agnarsson, I., 2009. Reconstructing web evolution and spider diversification in the molecular era. Proceedings of the National Academy of Sciences of the United States of America 106, 5229–5234.

Brignoli, P.M., 1972. Ragni de Ceylon I. Missione biospeleologica Aellen-Strinati (1970) (Arachnida, Araneae). Revue Suisse de Zoologie 79, 907–929.

Coddington, J., 1986. The monophyletic origin of the orb web. In: Shear, W.A. (Ed.), Spiders: Webs, Behavior, and Evolution. Stanford University Press, Stanford, pp. 319–363.

Czajka, M., 1963. Unknown facts of the biology of the spider *Ero furcata* (Villers) (Mimetidae, Araneae). Polskie Pismo Entomologiczne 33, 229–231.

Dimitrov, D., Hormiga, G., 2011. An extraordinary new genus of spiders from Western Australia with an expanded hypothesis on the phylogeny of Tetragnathidae (Araneae). Zoological Journal of the Linnean Society 161, 735–768.

Dimitrov, D., Lopardo, L., Giribet, G., Arnedo, M.A., Álvarez-Padilla, F., Hormiga, G., 2012. Tangled in a sparse spider web: single origin of orb weavers and their spinning work unraveled by denser taxonomic sampling. Proceedings of the Royal Society B 279, 1341–1350.

Forster, R.R., Platnick, N.I., Coddington, J., 1990. A proposal and review of the spider family Synotaxidae (Araneae, Araneoidea), with notes on theridiid interrelationships. Bulletin of the American Museum of Natural History 193, 1–116.

Gorb, S.N., Barth, F.G., 1996. A new mechanosensory organ on the anterior spinnerets of the spider *Cupiennius salei* (Araneae, Ctenidae). Zoomorphology 116, 7–14.

Griswold, C.E., 2001. A monograph of the living world genera and Afrotropical species of cyatholipid spiders (Araneae, Orbiculariae, Araneoidea, Cyatholipidae). Memoirs of the California Academy of Sciences 26, 1–251.

Griswold, C.E., Coddington, J.A., Hormiga, G., Scharff, N., 1998. Phylogeny of the orb-web building spiders (Araneae, Orbiculariae: Deinopoidea, Araneoidea). Zoological Journal of the Linnean Society 123, 1–99.

Griswold, C.E., Ramírez, M.J., Coddington, J.A., Platnick, N.I., 2005. Atlas of phylogenetic data for entelegyne spiders (Araneae: Araneomorphae: Entelegynae) with comments on their phylogeny. Proceedings of the California Academy of Sciences, 4th Series 56 (Suppl. II), 1–324.

Harms, D., Dunlop, J.A., 2009. A revision of the fossil pirate spiders (Arachnida: Araneae: Mimetidae). Palaeontology 52, 779–802.

Harms, D., Harvey, M.S., 2009a. A review of the pirate spiders of Tasmania (Arachnida, Mimetidae, *Australomimetus*) with description of a new species. Journal of Arachnology 37, 188–205.

Harms, D., Harvey, M.S., 2009b. Australian pirates: systematics and phylogeny of the Australasian pirate spiders (Araneae: Mimetidae), with a description of the Western Australian fauna. Invertebrate Systematics 23, 231–280.

Heimer, S., 1986. Notes on the spider family Mimetidae with description of a new genus from Australia (Arachnida, Araneae). Entomologische Abhandlungen, Staatliches Museum für Tierkunde, Dresden 49, 113–137.

Hickman, V.V., 1967. Some Common Tasmanian Spiders. Tasmanian Museum and Art Gallery, Hobart.

Jackson, R.R., Whitehouse, M.E.A., 1986. The biology of New Zealand and Queensland pirate spiders (Araneae, Mimetidae): aggressive mimicry, araneophagy and prey specialization. Journal of Zoology, London, Series A 210, 279–303.

Lopardo, L., Hormiga, G., 2007. On the synaphrid spider *Cepheia longiseta* (Simon 1881) (Araneae, Synaphridae). American Museum Novitates 3575, 1–18.

Mello-Leitão, C.F. de, 1935. Dois novos Mimetidae do Brasil meridional, com algumas notas sobre a familia. Annaes da Academia Brasileira de Sciencias 7, 323–327 (plus 2 plates).

Miller, J.A., 2007. Synaphridae of Madagascar (Araneae: Araneoidea): a new family record for the Afrotropical region. Proceedings of the California Academy of Sciences, 4th Series 58, 21–48.

Peters, H.M., 1987. Fine structure and function of capture threads. In: Nentwig, W. (Ed.), Ecophysiology of Spiders. Springer, Berlin, pp. 187–202.

Peters, H.M., 1993. Functional organization of the spinning apparatus of *Cyrtophora citricola* with regard to the evolution of the web (Araneae, Araneidae). Zoomorphology 113, 153–163.

Platnick, N.I., 2013. The World Spider Catalog, Version 13.5. American Museum of Natural History, New York. http://dx.doi.org/10.5531/db.iz.0001. Available from: http://research.amnh.org/iz/spiders/catalog (accessed 16.04.13.).

Platnick, N.I., Shadab, M.U., 1993. A review of the pirate spiders (Araneae, Mimetidae) of Chile. American Museum Novitates 3074, 1–30.

Scharff, N., Coddington, J.A., 1997. A phylogenetic analysis of the orb-weaving spider family Araneidae (Arachnida, Araneae). Zoological Journal of the Linnean Society 120, 355–434.

Schütt, K., 1995. *Drapetisca socialis* (Araneae: Linyphiidae): web reduction – ethological and morphological adaptations. European Journal of Entomology 92, 553–563.

Schütt, K., 2000. The limits of the Araneoidea (Arachnida: Araneae). Australian Journal of Zoology 48, 135–153.

Simon, E., 1895. Histoire naturelle des araignées, second ed., vol. 1. Librairie Encyclopédique de Roret, Paris.

Townley, M.A., Horner, N.V., Cherim, N.A., Tugmon, C.R., Tillinghast, E.K., 1991. Selected aspects of spinning apparatus development in *Araneus cavaticus* (Araneae, Araneidae). Journal of Morphology 208 175–191, C5–C7.

Townley, M.A., Tillinghast, E.K., Cherim, N.A., 1993. Moult-related changes in ampullate silk gland morphology and usage in the araneid spider *Araneus cavaticus*. Philosophical Transactions of the Royal Society of London, Series B 340, 25–38.

Townley, M.A., Tillinghast, E.K., 2003. On the use of ampullate gland silks by wolf spiders (Araneae, Lycosidae) for attaching the egg sac to the spinnerets and a proposal for defining nubbins and tartipores. Journal of Arachnology 31, 209–245.

Townley, M.A., Tillinghast, E.K., 2009. Developmental changes in spider spinning fields: a comparison between *Mimetus* and *Araneus* (Araneae: Mimetidae, Araneidae). Biological Journal of the Linnean Society 98, 343–383.